heritage

MDPI

Article

Prospection of the Red Biological Patinas Influencing the Urban Scenery Architecture in Portuguese Territory

Fabio Sitzia [1,*], Carla Lisci [1], Luis Dias [1], Silvia Macedo Arantes [1] and Ana Teresa Caldeira [1,2,3]

[1] HERCULES Laboratory & IN2PAST, University of Évora, Palácio do Vimioso, Largo Marquês de Marialva 8, 7000-809 Évora, Portugal; clisci@uevora.pt (C.L.); luisdias@uevora.pt (L.D.); saa@uevora.pt (S.M.A.); atc@uevora.pt (A.T.C.)
[2] Department of Chemistry and Biochemistry, School of Sciences and Technology, University of Évora, Rua Romão Ramalho 59, 7000-671 Évora, Portugal
[3] City U Macau Chair in Sustainable Heritage & Sino-Portugal Joint Laboratory of Cultural Heritage Conservation Science, Institute for Advanced Studies and Research, University of Évora, Largo Marquês de Marialva 8, 7000-809 Évora, Portugal
* Correspondence: fsitzia@uevora.pt

Abstract: Portugal's architecture reflects a rich history influenced by Roman, Moorish, Neoclassical and Romantic styles, with the 20th century marked by Art Deco and colonial influences. Regional styles vary, with white-painted buildings commonly experiencing color changes due to biofilm formation. Visually striking are the red-colored biological patinascommon in the coastal areas. A survey of 120 historical buildings affected by bio-colonization helps to understand the reasons for the patinas' growing, which beyond natural factors, is often linked to construction defects. A characterization of four samples utilizes Next-Generation Sequencing (NGS) to identify the microorganisms composing the red biofilm, while the SEM-EDS, FTIR-ATR and XRD techniques provide further insights into the biofilm and substrate features. The comprehensive data of biochemical characterization indicate a wide variety of microorganisms, including bacteria and fungi, some of which exhibit potential as producers of a UV-tolerant red/yellow pigment (carotenoid) responsible for the macroscopic coloration of bio-colonization.

Keywords: Next-Generation Sequencing; rural landscape; building pathology; commercial painting; relative humidity; climate; bio-deterioration

Citation: Sitzia, F.; Lisci, C.; Dias, L.; Arantes, S.M.; Caldeira, A.T. Prospection of the Red Biological Patinas Influencing the Urban Scenery Architecture in Portuguese Territory. *Heritage* **2024**, *7*, 7236–7254. https://doi.org/10.3390/heritage7120334

Academic Editor: Manuela Vagnini

Received: 3 October 2024
Revised: 3 December 2024
Accepted: 9 December 2024
Published: 16 December 2024

1. Introduction

Bio-colonization is a slow and constant process that affects all types of building materials [1,2]. It can induce biodeterioration or any modification, generally superficial, due to the activity of living organisms. Primarily, the consequences of biological colonization are chromatic alterations, patinas, stains and crusts.

In buildings, especially in outdoor environments, the main organisms responsible for bio-colonization are superior plants, lichens, bacteria, fungi and algae.

Studies on the characterization of superior plants' monument biodeteriogens are quite common in the literature because their growth causes damage due to the pressure exerted by roots [3,4]. On the contrary, biological patinas, particularly lichen and mosses, confer to the monuments a romantic antique aspect and beauty. Although their disruptive action against the stone substrate is known, this type of building pathology is often tolerated as evidence of the signs of time [5]. In addition, lichens and mosses do not induce structural damage by compromising the stability of the building [6]. Lichens derive from the symbiosis between a fungus and an alga or cyanobacteria. Their bio-decay action is given by the secretion of lichen acids (e.g., usnic, $C_{18}H_{16}O_7$; gyrophoric, $C_{24}H_{10}O_{20}$; pulvinic, $C_{18}H_{12}O_5$) [7,8]. The latter probably have an antibacterial and repulsive function against herbivorous animals [9].

Acid-secreted substances are chelating binders which act through the formation of complexes with metal cations from the growing substrate [5,10].

The biocorrosion process caused by lichens operates over an extensive timescale, ultimately contributing to the pedogenesis of the rocky substrate on which they grow [11].

Some fungi such as *Aspergillus* and *Penicillium* and bacteria such as *Bacillus* and *Pseudomonas* are known for their ability to produce oxalic acid during their metabolic cycle. This acid could interact with the calcium present in rocks, particularly limestones, forming calcium oxalate (CaC_2O_4) [12].

Bio-decay also occurs due to the action of sulfuric acid (H_2SO_4) produced by colonizing microorganisms such as bacteria (e.g., *Acidithiobacillus*, *Sulfolobus*, *Desulfovibrio*) and fungi (e.g., *Penicillium*, *Aspergillus).*

Sulfuric acid especially reacts with carbonate substrates (e.g., limestones, marbles, marls) and mortars. H_2SO_4 can create sulfate-based crusts (e.g., Gypsum $CaSO_4 \cdot 2H_2O$, or Mirabilite $Na_2SO_4 \cdot 10H_2O$) [13]. They can precipitate inside the pores of the stone and recrystallize, exerting a crystallization pressure that favors the disintegration of the stone.

The nitric acid (HNO_3) expelled by nitrifying bacteria (e.g., *Nitrobacter*, *Nitrospina*, *Nitrospira*) leads to the dissolution of the limestone and the formation of nitrate salts (e.g., Nitratine, $NaNO_3$) [14]. In addition to the purely chemical aspects, some microorganisms develop hyphae (filaments) that penetrate the micropores of the stone, causing fractures or detachment. The identification of the microbiota colonizing stone building materials of contemporary and ancient cultural heritage, as well as their relationships between climate and substrate, is the research subject of several scientific studies and projects [15,16].

Microbial activities are governed by thermo-hygrometric conditions [17]. Generally, biofilm formation, community composition and species assortment are mainly influenced by water availability. Studies have indicated that alterations in phototroph biomass may occur in response to changes in water availability [18]. Subsequent investigations have identified moisture as a potential key factor. Although a direct relationship was not observed, researchers have hypothesized that biofilm distribution may be influenced by the temporal occurrence of moisture and the resulting transient wetting events, as well as the duration of these events [19].

Any significant variation in the thermo-hygrometric features and the atmospheric concentrations of SO_X NO_X, CO_2, CO and particulate matter can modulate the development of biological communities [17].

This research characterizes very common red biological patinas found on buildings in southern and coastal Portugal, commonly known as '*Trentepohlia*', a genus of filamentous green algae of chlorophyte family. As we will observe in the results, the patina under investigation is biologically much more complex, with chlorophyte making up only a small portion.

The biofilm under study is typically located in white-painted buildings whose color is due to various reasons related to culture, climate and local tradition.

In addition to providing a clean, uniform appearance, white paints also help reflect sunlight, reducing heat absorption and keeping interiors cooler.

Furthermore, the Moorish presence in Portugal, which dominated parts of the Iberian Peninsula until the 13th century, strongly influenced architectural traditions, including the use of white varnish. In the past, the white color of Portuguese houses was obtained by the whitewashing technique. It refers to a traditional technique, often seen in Mediterranean, Colonial, and rural areas, where the exterior walls are coated with a thin layer of whitewash (a mixture of lime, water, and sometimes other materials like chalk).

Today, whitewashing has fallen into disuse, with synthetic white paints being used instead.

The difference between these two finishes is remarkable.

Lime paints are ideal for ecological projects or historical restorations due to their natural breathability, traditional aesthetics, and low environmental impact, although they require constant maintenance.

Modern synthetic paints are cheaper and more resistant to weathering; however, they can limit the breathability of surfaces and have a negative environmental impact. Unlike lime, they have less biocidal properties.

This is why the white modern buildings in these areas, depending on their location, orientation, and climate conditions, only maintain their white appearance for 2–3 years and after that, the paint is affected by black, green and especially red biological patinas (Figure 1). The latter has always aroused interest in the local population, especially due to the strong red color that, on a white surface, points out a notational color distance (CIE76) Δ_{ab} = ~60, a considerable value if compared to the human limit detection, attested at around 5 [20]. According to our observations and compared to other green or black biofilms, the red patina has considerable bio-colonizing potential with the ability to cover entire buildings in a few years.

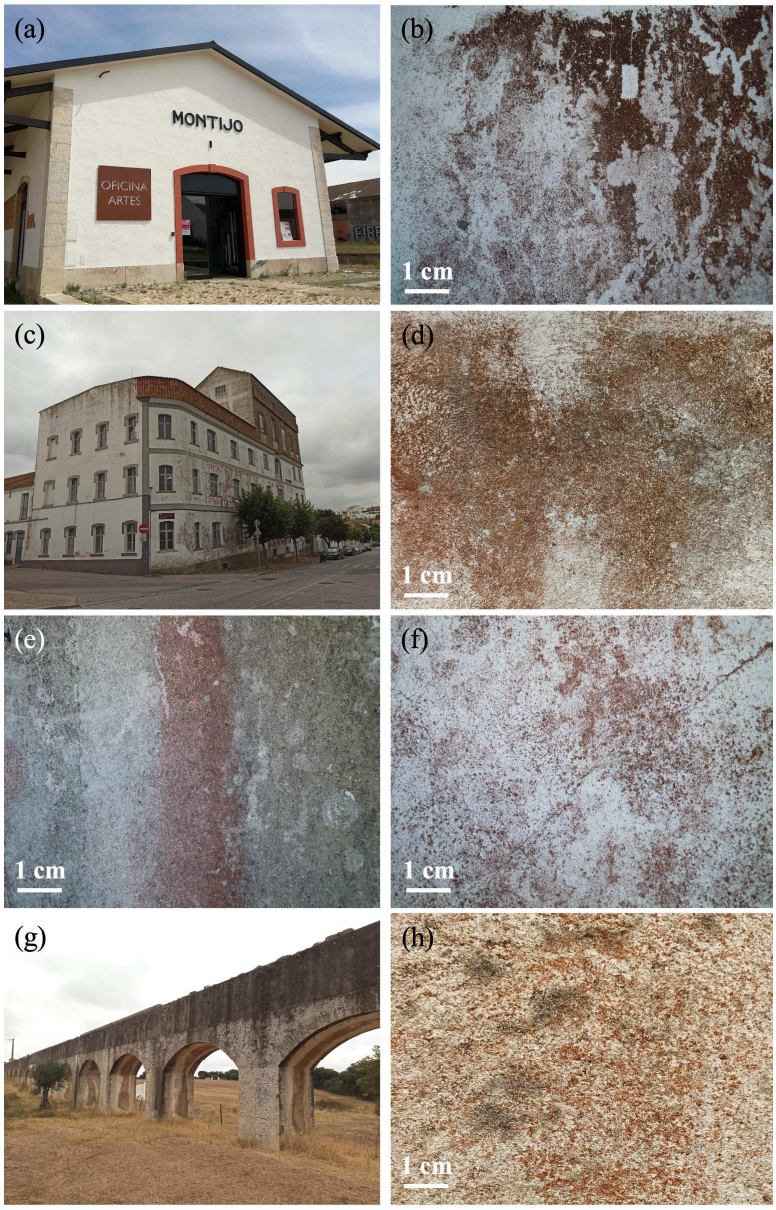

Figure 1. The four buildings affected by biological patina and the objects of this study: (**a**,**b**) Ancient train station (*Montijo*, Portugal) and red patina affecting the building. (**c**,**d**) Old grinding factory and red patina affecting the building (*Arraiolos*, Portugal). (**e**,**f**) Snapshots of red biological patina affecting an ancient private house in *Alcochete* (Portugal). The building is not shown for privacy reasons, (**g**,**h**) Ancient aqueduct (*Évora*, Portugal) and relative red patina.

The presence of this type of biological patina, even if situated outdoors, can affect the interior environment of the house by diminishing the walls' ability to manage rainwater runoff, retaining moisture, and reducing the breathability of the building envelope. As a result, the indoor environment becomes more humid by promoting the growth of indoor biological patinas, some of which can be harmful to health.

In this study, a high-throughput sequencing approach was performed on these red patinas to identify the composing microorganisms.

Scanning Electron Microscopy (SEM) was used to characterize the substrate. Fourier-Transform Infrared Spectroscopy (FTIR) was selected as the methodology able to detect the patina composition and the eventual organic substance secreted.

Diagnosing the building envelope helps to identify the causes of patina growth, which is often linked to both construction defects and environmental factors. This problem is underscored by the annual global financial losses and health issues caused by the biological deterioration of stone buildings and structures [21].

2. Materials and Methods

2.1. Materials

The field survey and building pathology analysis were conducted on 120 buildings, most of them located within the historic centers of *Sesimbra*, *Alcochete*, *Montijo*, *Alcáçer do Sal*, *Setúbal*, *Fátima*, *Caldas da Rainha*, *Évora*, and *Arraiolos*. As part of these historic centers, the facilities are protected to preserve their historical, artistic, and environmental significance. From this group of 120 buildings, four of them, which present historical and architectural importance, and which present sampleable traces of biofilm, were selected for further study (see Table 1 and Figure 1).

Table 1. Sampling information about the red collected patinas.

Sample	Building Information	Coordinates	Growing Substrate	Wall Exposition of Sampling Point
L1	Ancient train station (*Montijo*) Year: 1908 Last painting's year: 2008	38°42′6.58″ N 8°58′16.13″ O	Lime rendering with traces of synthetic white varnish	NNE
L2	Old grinding factory (*Arraiolos*) Year: 1900–1920 Last painting's year: 2009	38°43′21.75″ N 7°59′5.05″ O	Synthetic white varnish	NNW
L3	Ancient private house (*Alcochete*) Year: 1895 Last painting's year: 2010	N/A	Synthetic white varnish	NNW
L4	Ancient aqueduct (*Évora*) Year: 1873–1879 Last painting's year: Unknown	38°36′41.88″ N 7°57′1.95″ O	Lime rendering with traces of synthetic white varnish	NNW

The first selected building is the ancient train station of *Montijo*, originally called *Aldegallega*, which was a railway interface of the *Montijo* Branch. Having started operating in 1908, the *Montijo* Branch had a length of 10.6 km and in 1927 was integrated into the *Companhia dos Caminhos de Ferro Portugueses* (Lisbon, Portugal) with the intention of transporting goods and passengers [22]. Traffic on the branch was suspended in 1989, mainly due to economic reasons [22].

The second building taken into consideration is the old grinding factory in *Arraiolos* built between 1900 and 1920 [23]. The building stands in the center of the town of *Arraiolos* and is today only partly used for feed production. In the past, it had several uses, although it was initially used for grinding grain.

For the third building under study, no information is available other than the construction date of 1895.

The Águeduto da Prata in *Évora*, inaugurated on 28 March 1537, was constructed in just six years under the supervision of royal architect Francisco de Arruda, commissioned by King João III [24]. Spanning approximately 18 km, it originally transported water from the *Herdade da Prata* in the *Arraiolos* municipality to *Évora*, likely following the path of an ancient Roman aqueduct. After sustaining damage during wars, it was reconstructed between 1873 and 1879 [24]. Today, the aqueduct, still over 18 km long, brings water from the nearby village of *Graça do Divor.*

Following the construction, all four buildings underwent numerous renovations and were repainted several times using contemporary paints, often of low quality.

In the buildings, biological samples and the respective substrate were extracted at an elevation of about one meter from the ground by using sterile plastic scrapers. The samples were placed in sterile containers and stored at a constant temperature of 4 °C until further processing.

In addition to the patina, paint substrate fragments of approximately 4 cm^2 in size were collected.

2.2. Methods

2.2.1. SEM-EDS, FTIR-ATR, XRD Analysis and Field Survey

For the elemental characterization of substrates, a SEM S-3700N VP (Hitachi, Tokyo, Japan) with Bruker Xflash Quantax Compact Plus 630M detector (Bruker, Billerica, MA, USA) was utilized.

For the mineralogical analysis of the substrate, an AXS D8 Discover XRD (Bruker, Billerica, MA, USA) with a CuKα source, operating at 40 kV and 40 mA, and a Lynxeye 1-dimensional detector were used. Scans were performed from 3 to 75° 2θ, with 0.05° 2θ step, and 1 s/step measuring time by point. Diffract-Eva software version 6 from Bruker with the PDF-2 mineralogical database (International Centre for Diffraction Data—ICDD) was used to identify the peaks.

The color measurements of the patinas were carried out by a portable DataColor Check Plus II spectrophotometer (DataColor, Lawrenceville, NJ, USA) and are reported according to the CIE L*a*b* color space.

Analysis by Infrared Spectroscopy was performed with the help of an Alpha spectrometer, from Bruker Optics (Ettlingen, Germany), with the Total Attenuated Reflection (ATR) module. The OPUS version 6.5 Bruker® software was used for the processing and treatment of the spectra. IR spectra were traced in the region with a scale between 4000 and 375 cm^{-1}, with 128 scans and a spectral resolution of 4 cm^{-1}.

2.2.2. High-Throughput Sequencing (HTS)

To evaluate the microbial population in the samples from the four selected locations (L1, L2, L3, and L4), environmental DNA (eDNA) was extracted using the NZYSoil gDNA Isolation Kit (NZYTech, Lisboa, Portugal), following the manufacturer's protocol. The extracted DNA was quantified via spectrofluorimetry using the QuantiFluor® One dsDNA System (Promega, Madison, WI, USA) and a Quantus™ fluorometer (Promega, Madison, WI, USA).

After DNA extraction and quantification, the samples were used to amplify the ITS2 region for eukaryotes and the 16S rDNA V3-V4 subunit for prokaryotes. The analytical procedure followed previously established methods for studying microbial diversity in environmental samples [25,26].

All analyses were performed in triplicate. Heatmaps were generated using data normalized by the total sum scaling (TSS) method in MicrobiomAnalyst [27]. Samples were grouped based on type, allowing for the visualization of patterns and similarities across groups. TSS normalization was applied to ensure comparison among samples by adjusting the relative

proportions of abundances. This approach highlights specific variations between sample types, illustrated by the differences in color intensity on the heatmap.

3. Results and Discussion

3.1. Building Pathology and Climatic Context Associated with the Patina

This section will show some of the 120 case studies of buildings affected by the red biofilm.

It is found on surfaces with high water content from run-off, condensation, humidity, or hygroscopic materials and sufficient time of wetness. Its colonization is consistent, and after removal, it regrows, creating distinctive red streaks that stain clean walls. In the survey of the 120 buildings, red biofilms were mainly found on walls facing NW and NNW, the directions of the prevailing winds (Figure 2a,b). Along Portugal, NW winds (*Nortada*) are common from May to September and are responsible for the transport of humidity from the sea, especially in coastal areas. This is one of the first reasons linking patina growing to wind direction. Other potential reasons could involve the microorganisms within the patina positioning themselves strategically toward wind direction to optimize spore dispersion, thereby enhancing their ability to colonize new areas.

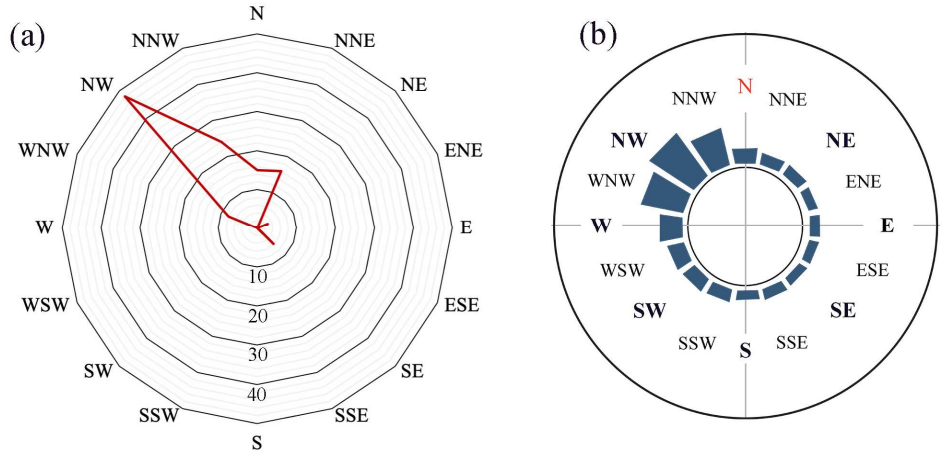

Figure 2. (**a**) Cardinal exposition of the wall stained by the red patina. A total of 120 buildings located in the villages of *Sesimbra*, *Alcochete*, *Montijo*, *Alcacer do Sal*, *Setubal*, *Fatima*, *Caldas da Rainha*, *Évora* and *Arraiolos* were considered for the observations; (**b**) direction and frequency of the winds in the study areas.

As regards Figure 2a, SE-exposed walls are slightly prone to colonization. This only happens when tall adjacent buildings cast their shadow on the patina during a significant portion of the year. Red bio-colonization grows on overhanging surfaces and does not affect surfaces with deposits of copper oxides. These are generally due to rainwater leaching of copper elements such as anchors and epitaphs. It is already known how copper oxides act as a bio-inhibitor [28].

The climate and the moisture content of the air are crucial for the growth of the red patina. In coastal areas, where humidity is highest, about 60% of buildings that have been painted from more than 2–3 years with synthetic varnish show signs of bio-colonization. In inland areas with lower humidity rates, bio-colonization is practically absent or in percentages of less than 1% of the buildings.

In addition to synthetic varnishes, this colonization can easily be detected on limestones and marbles utilized in local vernacular architecture [29]. The patina is also responsible for different types of building pathologies and indicates different causes of damage. The most representative are as follows:

Red streaks: They appear in walls subjected to seepage and direct wetting from rainwater. These stained streaks appear primarily due to the vertical runoff growth of

colonies forced by gravity (Figure 3a). The staining process occurs as the pigmented cells of the algae embed and adhere to the surface, resulting in lasting marks.

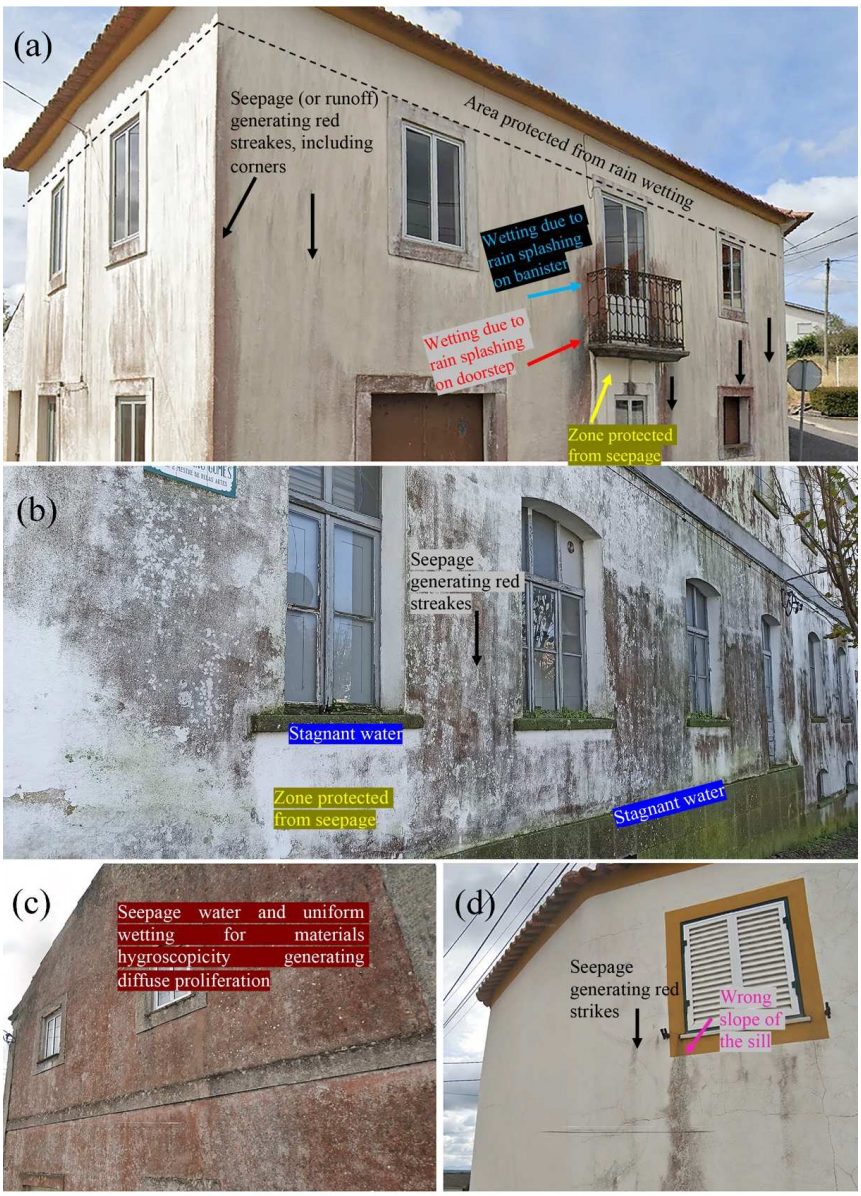

Figure 3. Practical cases of bio-colonization as markers of building pathologies: (**a**,**c**,**d**) private houses, (**b**) old grinding factory (*Arraiolos*), sampling location of the specimen L2.

Diffuse patinas on plasters and renders: These appear as widespread and homogeneous colonization on the whole surface, both for diffuse runoff and for the natural hygroscopicity of the materials (Figure 3b,c). A complete bio-colonization like the one shown in Figure 3c can occur after about 10 years from the last painting.

Infiltrative phenomena due to construction defects such as wrong slopes of the sill, lack of sealant, etc., could be responsible for biofilm formations (Figure 3d).

Ghost effect, *ghosting or thermal tracking*: Ghosting consists of the outline of the blockwork shown through the render as a result of penetrating dampness from the underlying masonry with different wettability properties and thermal conductivity, generating structural thermal bridging [30]. Dry areas typically experience greater heat dispersion, such as in reinforced concrete structures. Consequently, surfaces in these areas tend to be warmer, facilitating quicker evaporation of water and moisture and thereby preventing mold formation. Conversely, thermally insulated areas do not promote rapid water evaporation,

allowing for the buildup of moisture and facilitating mold growth and other biological activities [31], (Figure 4a,b).

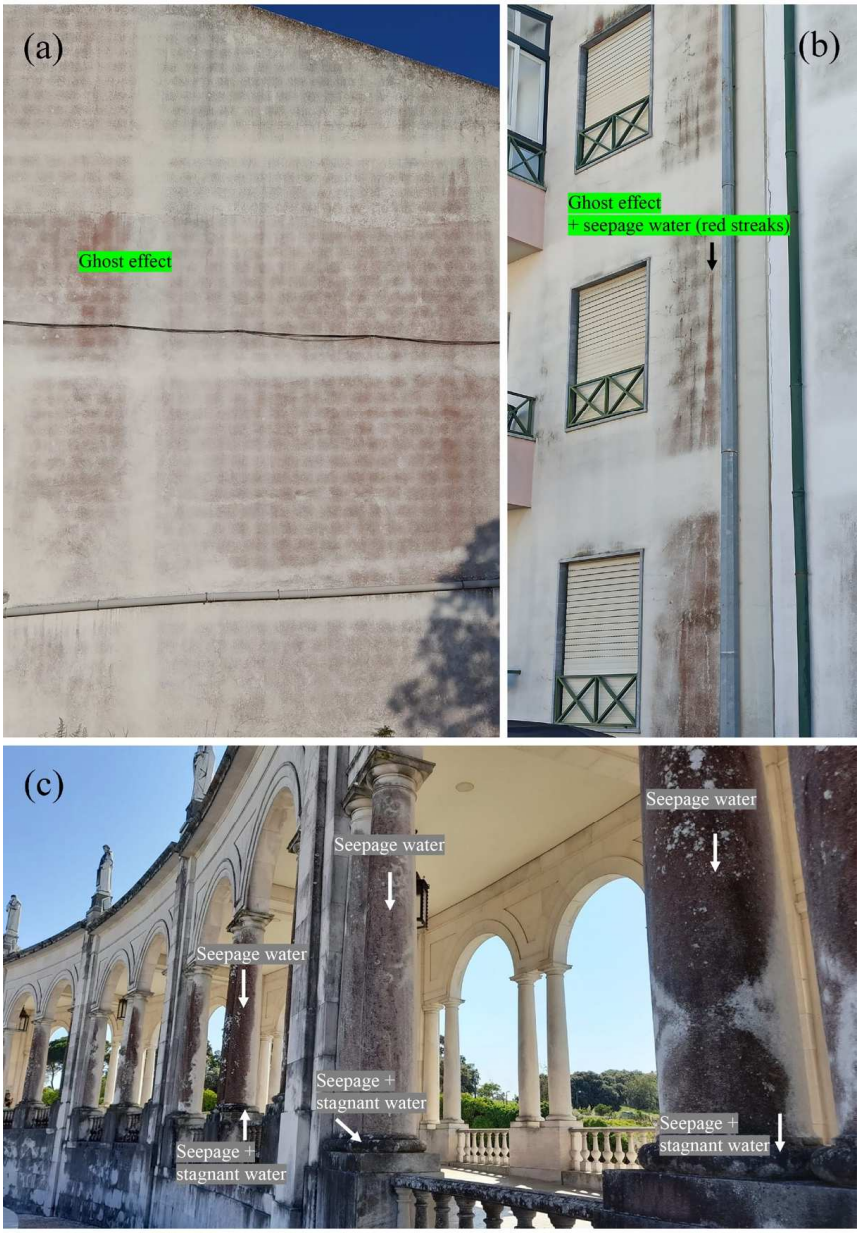

Figure 4. Practical case of bio-colonization as markers of building pathologies: (**a**,**b**) private buildings, (**c**) colonnade at Fatima's sanctuary.

Ghosting can be considered as a chromatic alterations in facades able to highlight, positively or negatively, the structural frame and building component [32].

Others: colonization induced by wetting due to rain splashing and stagnant water (Figure 4c).

3.2. Chemical and Macroscopic Characterization of Patina and Substrate

The four bio-colonization samples have a characteristic red color whose intensity is based on the thickness of the biofilm. During the early stages of growth, when thickness is of less than 0.5 mm, the patina has a pinkish color, in which the red-regulating component (a*) in the CIE L*a*b* color space is around 5. With thicknesses larger than 1 mm, an a* component of around 10 is achieved. In the case of thicker and older bio-colonization, the red color is noticeable and the a* component can draw values above 20.

Normally, the patina starts having a pink color in the early stages of growth where the L-component is also relatively high (up to 70) and reaches a darker burgundy color with an L-component of about 20 in about 10 years. Biofilms can be mechanically removed by rubbing with the finger. After this operation, the patina changes color, leaving a yellow powder on the fingers.

FTIR-ATR analysis was executed to identify the functional group characteristic of the biological patina [33,34] (Figures 5 and 6, Table 2).

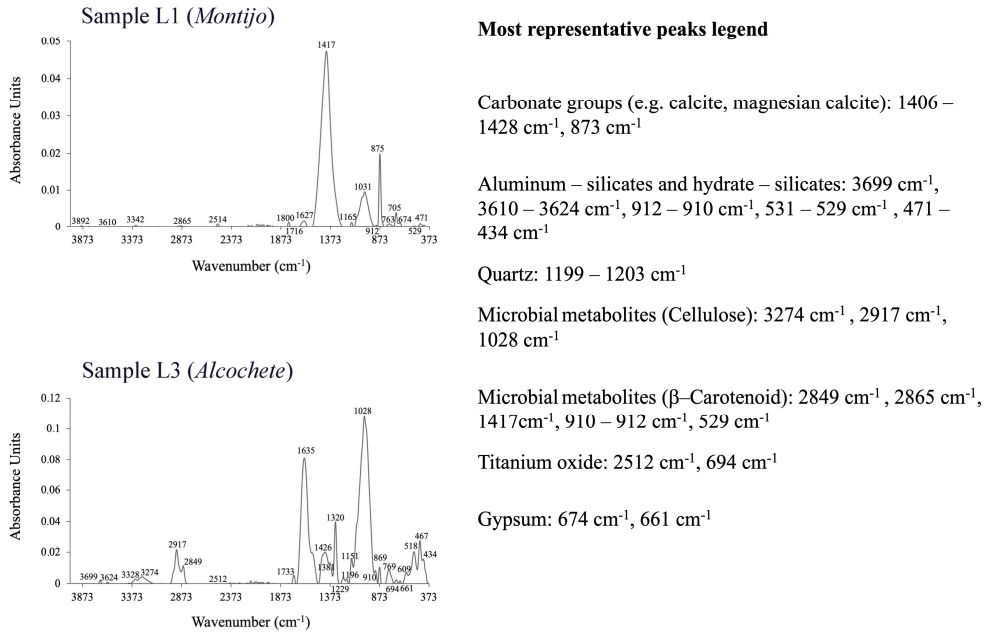

Figure 5. FTIR-ATR survey on biofilms from *Montijo* and *Alcochete*.

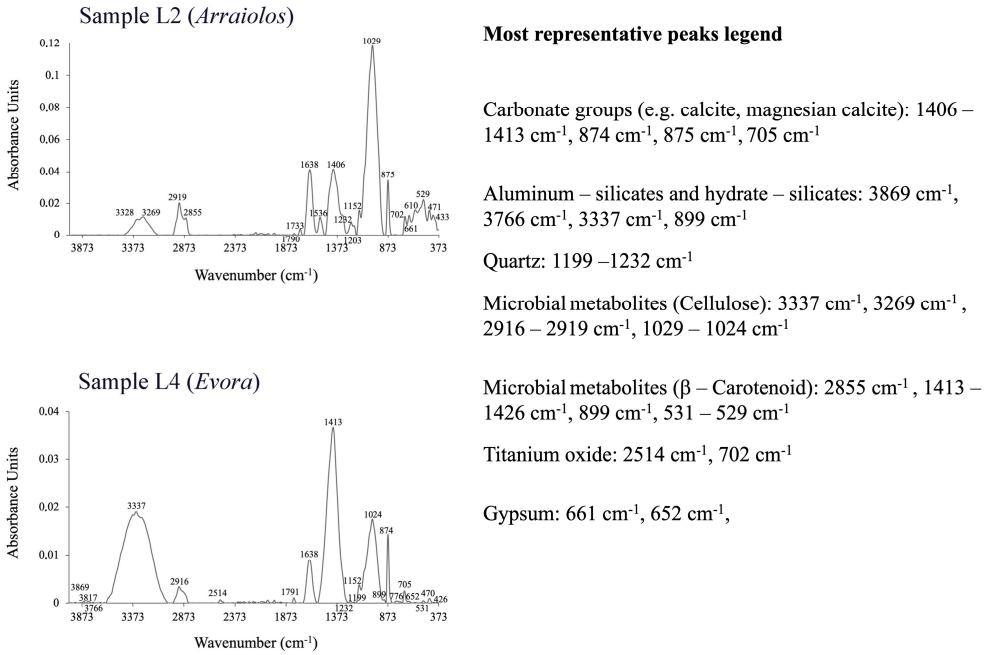

Figure 6. FTIR-ATR survey on biofilms from *Arraiolos* and *Évora*.

Table 2. Summary of the main features of patinas and substrates, as shown in Section 3.2.

Sample Information	Biological Patina		Paint Substrate	
	Color (CIE L*a*b*)	**FTIR-ATR Results**	**Elemental Composition (Mass. Norm. %)**	**Mineralogical Composition (Wt %)**
L1 Ancient train station (*Montijo*) Year: 1908 Last painting's year: 2008	21*8*11*	Calcite Silicates Sulfates Organic compounds (cellulose and carotenoids)	C 11.8 O 53.60 Mg 1.08 Ca 33.09 Na 0.17 Al 0.29 Si 0.44 S 0.17 Cl 0.08	Calcite 100
L2 Old grinding factory (*Arraiolos*) Year: 1900–1920 Last painting's year: 2009	32*10*15*	Calcite Silicates Organic compounds (cellulose and carotenoids)	C 8.08 O 50.73 Mg 2.30 Ca 37.49 Na 0.24 Al 0.29 Si 0.88	Calcite 100
L3 Ancient private house (*Alcochete*) Year: 1895 Last painting's year: 2010	66*8*5*	Calcite Silicates Titanium oxides Sulfates Organic compounds (cellulose and carotenoids)	C 7.88 O 48.11 Mg 0.62 Ca 29.21 Ti 12.34 Na 0.16 S 0.37 Al 0.50 Si 0.81	Calcite 60,6 Rutile 13 Gypsum 24.2 Quartz 2.2
L4 Ancient aqueduct (*Évora*) Year: 1873 Last painting's year: Unknown	45*22*27*	Calcite Silicates Sulfates Titanium oxides Organic compounds (cellulose and carotenoids)	C 4.64 O 52.14 Mg 9.9 Ca 23.86 Fe 1.46 Ti 0.13 Cu 0.53 S 0.24 K 0.33 S 0.37 Al 2.74 Si 4.04	Magnesian calcite 100%

During sampling operations, it is very likely that some of the substrate was extracted along with the patina.

Carbonate groups referring to portions of the substrate are visible in different wavenumber ranges of frequencies (cm^{-1}). Inorganic C-O bonds of calcite and magnesian calcite related to the composition of the lime-based paintings are at about 1406–1426 cm^{-1}. Their position is approximately halfway between the typical wavenumbers for C=O double bonds and C-O single bonds. Since the carbonate group in inorganic compounds is planar, both in-plane and out-of-plane C-O bending vibrations occur. In general, the out-of-plane bending appears between 869 and 875 cm^{-1}, and the in-plane bending can be detected at around 702–705 cm^{-1}.

The presence of quartz (Si-O-Si chains) is detected at 1199–1203 cm^{-1} frequencies and the stretches at about 3699 cm^{-1}, 3610–3624 cm^{-1}, 899–915 cm^{-1} are indicative of the presence of Na-Mg aluminosilicates or other hydrate-silicates (Si-OH stretch) [33,34]. These

groups could refer to mineral additives of the substrate, mistakenly extracted along with the patina, or dust deposited on the surface.

At 518 cm^{-1}, 531–529 cm^{-1}, the frequency of Na-Al silicates [34] is also recognized.

Other inorganic compounds are present at 674 cm^{-1} and 655–661 cm^{-1}, which are the frequencies representing the gypsum [33]. Sulfates probably come from the marine aerosols in the *Montijo* and *Alcochete* villages. Sulfation of the carbonate-based painting can occur in the varnish of the *Évora* aqueduct.

Titanium and Titanium oxide used as anti-microbial in the paintings is detected both by SEM-EDS up to 12.34% (*Alcochete*, Table 2) and FTIR-ATR by the peaks at 3000 cm^{-1}, 2500–2600 cm^{-1}, 2200–2100 cm^{-1} and 700 cm^{-1}.

C=O stretching regarding organic compounds is detected at 1791–1800 cm^{-1} and 1733 cm^{-1} [33]. These compounds can be associated with the organic components of the paintings.

The compounds cellulose and β-carotenoids are products of the metabolic activity of the microorganism. Cellulose is at about 3269–3274 cm^{-1} (OH stretching), but it can also be detected at 2919–2016 cm^{-1}(C-H functional group), 1203–1151 cm^{-1} (C-C stretching), 1024–1031 cm^{-1}, 912 cm^{-1}–702 cm^{-1} and 674 cm^{-1} (C-OH/C-O-C stretching). β-carotenoids' infrared absorption frequencies can be determined at 2849–2855 cm^{-1} (C-H functional group), 1406–1426 cm^{-1} regions, 912–899 cm^{-1}, 531–529 cm^{-1} frequencies, and, finally, in the range of 661–652 cm^{-1} [34,35].

As mentioned above and indicated in Table 2, the substrate consists of synthetic white paint. EDS analysis demonstrates a composition consisting predominantly of calcium (23.86 < Ca < 37.49 Mass. Norm. %), oxygen (48.11 < O < 53.60 Mass. Norm. %) and carbon (4.64 < C < 11.8 Mass. Norm. %). These indicate a substrate mainly composed of calcite ($CaCO_3$), as detected by XRD. At the *Évora* aqueduct, the substrate appears to be magnesian calcite. Powder calcite is a pigment used to impart whiteness to the paint. It often happens that sulfation processes involve older varnishes, leading to the formation of gypsum.

The presence of other elements, such as sodium, aluminum, silicon and potassium, can be attributed to the paint and, with less probability, to render traces remnants on it. In many cases, the paint is degraded with clear phenomena of disintegration and exfoliation where small 'stratigraphic windows' show the underlying old paint or the rendering. This commonly includes quartz-feldspathic sands.

3.3. Microbial Communities

3.3.1. Procaryotic Communities

Regarding the analysis of bacterial communities, the most abundant phyla detected in the patinas concern proteobacteria (54%), actinobacteria (23%), firmicutes (10%) and cyanobacteria (7%).

As observed in the results, the macroscopic red color of the biofilm could be attributed to carotenoid pigments secreted by *Rubrobacter*, *Arthrobacter*, *Rosemonas, Rubellimicrobium*, and *Truepera* (Figure 7). These pigments serve various functions, including protection against harmful environmental factors such as UV radiation, oxidative stress, and competition from other microorganisms. Additionally, carotenoids are implicated in cell signaling, biofilm formation, and nutrient acquisition, which are critical for microbial survival in harsh environments.

Rubrobacter, predominant in L1 (*Montijo*) and L3 (*Alcochete*), is a genus known for its thermophilic and radiation-resistant species, and it is commonly associated with extreme environments, including high UV exposure and desiccation. Its ability to produce carotenoids contributes significantly to its resilience in such conditions. Studies have shown *Rubrobacter* species on cultural heritage sites, highlighting their role in biofilm formation and pigmentation [36,37]. Similarly, *Truepera*, found abundantly in L1 and L3 samples, is a radiation-resistant genus associated with pigment production. Its carotenoids protect against oxidative damage and contribute to biofilm pigmentation, particularly in exposed environments [38,39].

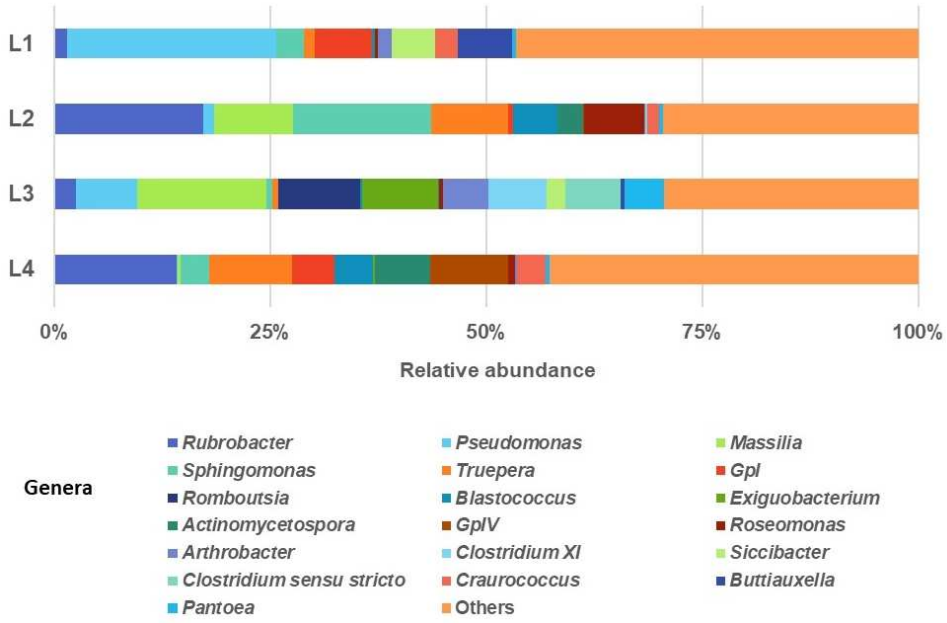

Figure 7. Relative abundance (%) of the majority genera present in the Procaryotic population.

Present mainly in L3, *Roseomonas* is characterized by its pink-to-red pigmentation, and it is frequently found in soil and water environments and occasionally in clinical settings. The production of carotenoids in *Roseomonas* provides protection against environmental conditions. Its ability to colonize surfaces and form biofilms suggests a role in the pink coloration observed on walls and stone materials [40,41]. *Sphingomonas* is another contributor to pigmentation. It is commonly found in oligotrophic environments and forms biofilms on diverse surfaces, including walls and stones [42].

Arthrobacter is widely distributed in soil, water, and air, and is known for its versatility and adaptability to environmental stresses. The genus is also a prolific producer of carotenoid pigments, which provide oxidative stress resistance and enhance its survival in fluctuating environments [43,44]. *Rubellimicrobium*, typically found in soil, marine environments, paper mills, and air, is common in coastal zones and contributes to marine biogeochemical cycles. This bacterium has also been documented on marbles, often in association with *Truepera*, *Aliterella*, and *Gloeocapsopsis*, indicating its role in biodeterioration and pigment production on stone surfaces [45].

The heat map for the prokaryotic populations (Figure 8) shows the top 58 abundant genera in the bacterial communities of the L1, L2, L3, and L4 samples. The four samples present distinct relative abundance profiles. The relative abundances of the genera *Gp16*, *GpXIII*, *Actinomyces*, *Rubellimicrobium*, *GpIV*, *Actinoplanes*, *Asticcacaulis*, *Solirubrobacter*, *Planomicrobium*, *Salmonella*, *Nitrolancea*, and *Actinomycetospora* are significantly higher in sample L1 (*Montijo*). The relative abundances of the genera *Clostridium_XI*, *Clostridium_sensu_stricto*, *Psychrobacter*, *Romboutsia*, *Pantoea*, *Exiguobacterium*, *Escherichia_shigella*, *Erwinia*, *Arthrobacter*, *Massilia*, *Bacillus*, *Enterobacter*, and *Acinetobacter* are significantly higher in sample L2 (*Arraiolos*). The relative abundances of the genera *Sphingobium*, *Roseomonas*, *Sphingomonas*, *Chlorophyta*, *Heliothrix*, and *Brevundimonas* are considerably higher in sample L3 (*Alcochete*). The relative abundances of the genera *Stenotrophomonas*, *Pseudomonas*, *Kluyvera*, *Raoultella*, *Sanguibacter*, *Citrobactrer*, *Siccibacter*, *Luteimonas*, *Geminicoccus*, *Euzebya*, *Promicromonospora*, *Buttiauxella*, and *Aquisphaera* are significantly higher in sample L4 (*Évora*).

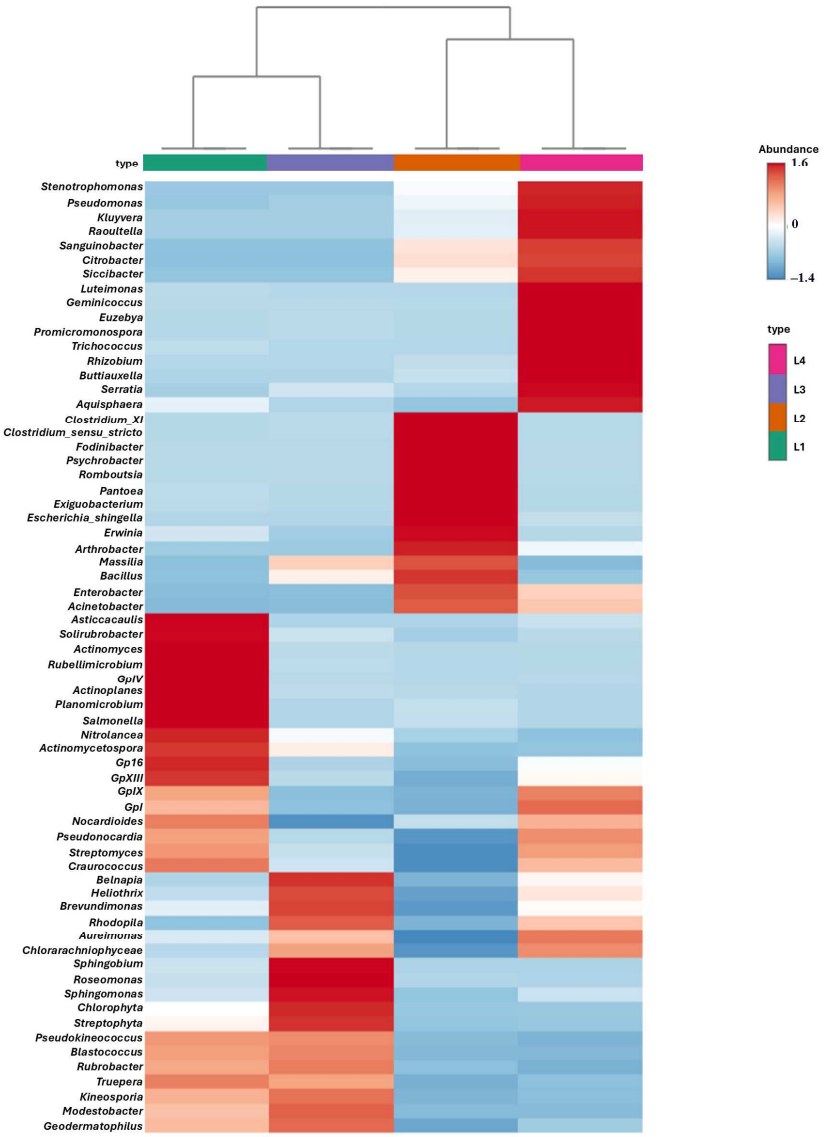

Figure 8. Heatmap analysis of the genera's relative abundance of every genus level based on the bacterial community 16s rDNA sequence, according to the average frequency of samples L1 (*Montijo*), L2 (*Arraiolos*), L3 (*Alcochete*) and L4 (*Évora*). Red and blue colors show the high and low enrichment of a genus, respectively. The scale represents normalized abundance values, where positive values indicate abundances above the mean and negative values indicate abundances below the mean relative to the dataset. These differences are visually represented by the color intensity on the heatmap.

The microbial composition analysis reveals that the samples from *Alcochete* and *Montijo* group into one cluster, while those from *Évora* and *Arraiolos* form a distinct cluster. This clustering likely reflects environmental and geographical factors influencing the microbial communities.

Alcochete and *Montijo* are geographically closer, sharing similar coastal and estuarine conditions, which may drive the selection of comparable microbial taxa adapted to such environments. In contrast, *Évora* and *Arraiolos*, located inland, are subject to distinct environmental pressures such as higher temperatures, lower humidity, and different substrate compositions, fostering a unique microbial assemblage.

These results suggest that local environmental conditions, including climate, substrate type, and human influence, play a critical role in shaping the microbial diversity.

The presence of pigment-producing microorganisms highlights the complex microbial interactions within biofilms. These genera not only play a role in pigmentation but also contribute to the biodeterioration of surfaces, particularly in environments exposed to intense environmental stressors such as high UV radiation and fluctuating humidity. Understanding the ecological and metabolic roles of these microbes can inform conservation strategies for preserving cultural heritage and managing microbial growth on architectural surfaces.

3.3.2. Eucarya Communities

The results show that the fungal population present in the collected biofilms belongs mostly to the phyla Ascomycota (96%) and Chlorophyta (3%).

The analysis reveals differences in the relative abundances of fungal genera across the samples (Figure 9). The genera *Caloplaca*, *Flavoplaca*, *Rinodina*, *Trebouxia*, *Vermiconia*, *Verrucaria*, *Incertomyces*, and *Lecania* are dominant in sample L1 (*Montijo*). Among these, certain genera like *Caloplaca* and Verrucaria are known to include lichen-forming species capable of producing carotenoids and other pigments contributing to red or orange biofilm pigmentation [46,47].

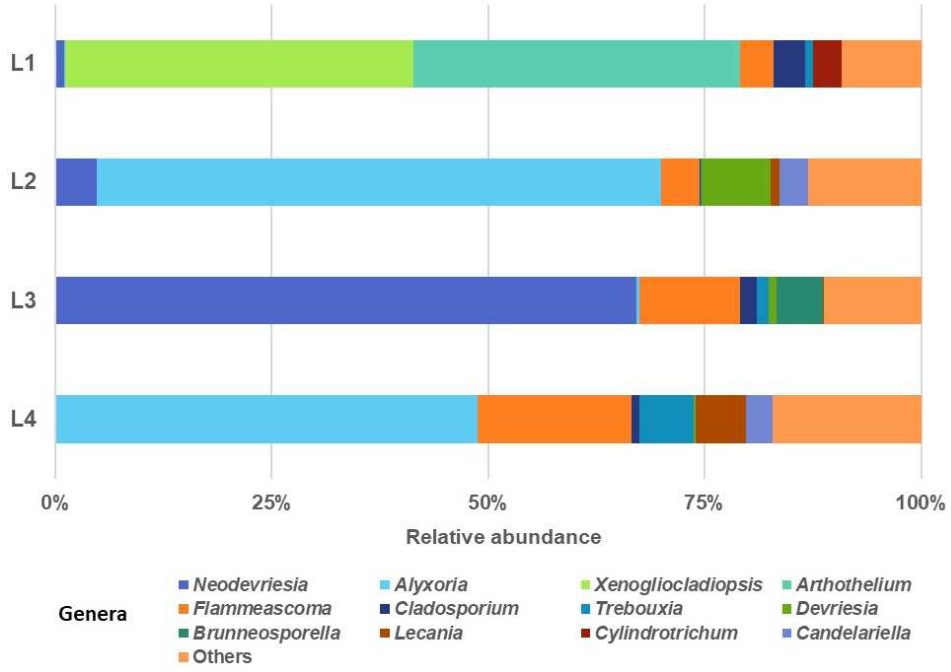

Figure 9. Relative abundance (%) of the majority phyla present in the eukaryotic population.

In sample L2 (*Arraiolos*), genera such as *Didymella*, *Megaspora*, *Brunneosporella*, *Phaeophyscia*, *Neodevriesia*, *Vishniacozyma*, *Mycosphaerella*, and *Calostilbe* dominate. Genera like *Neodevriesia* and *Vishniacozyma* are notable for their pigment production, including melanin and carotenoid derivatives, which could contribute to variations in pigmentation [48,49].

For sample L3 (*Alcochete*), the genera *Camarosporula*, *Devriesia*, *Capnobotryella*, and *Readeriella* are prevalent. Among these, *Devriesia* is particularly interesting due to its known ability to produce pigments, which may include carotenoids with reddish hues.

In sample L4 (*Évora*), a wider range of genera are present, including *Kazachstania*, *Alternaria*, *Athothelium*, *Xenogliocladiopsis*, *Cylindrotrichum*, *Stibella*, *Coniosporium*, *Tetracladium*, *Thelidium*, *Maasoglossum*, *Hirsutella*, *Polyblastia*, *Stemphylium*, *Acremonium*, *Ciphellophora*, and *Cladosporium*. Genera such as *Alternaria*, *Cladosporium*, and *Stemphylium* are notable for producing secondary metabolites, including pigments, which can range from melanin to carotenoid-like compounds [48,49].

In heatmap analysis (Figure 10), samples from *Alcochete* (L3) and *Montijo* (L1) form a cluster, while *Évora* (L4) and *Arraiolos* (L2) group into another cluster. This clustering

aligns with observations made in the bacterial communities discussed earlier in this article. The geographical proximity and environmental similarities between *Alcochete* and *Montijo*, including coastal influences and higher humidity levels, likely contribute to the shared microbial profiles [48]. Conversely, *Évora* and *Arraiolos*, located inland, experience drier conditions and different substrate compositions, which shape distinct fungal communities [47,48].

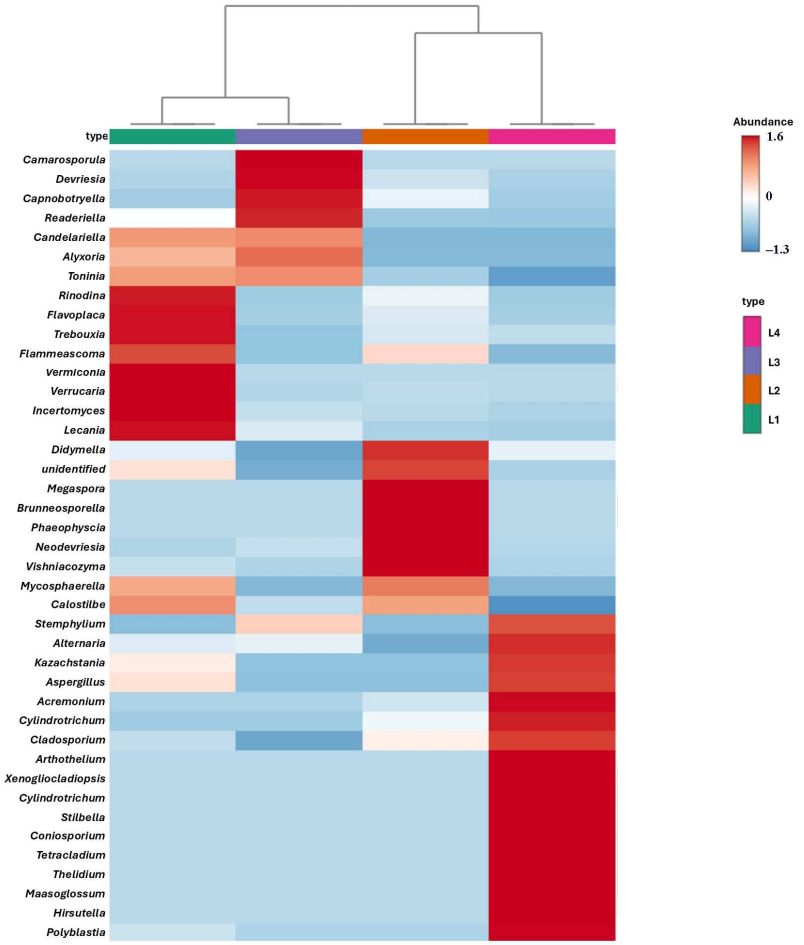

Figure 10. Heatmap analysis of the species relative abundance of every genus level based on the eucarya community ITS2 sequence, according to the average frequency of samples L1 (*Montijo*), L2 (*Arraiolos*), L3 (*Alcochete*), and L4 (*Évora*). Red and blue colors show the high and low enrichment of a genus, respectively. The scale represents normalized abundance values, where positive values indicate abundances above the mean and negative values indicate abundances below the mean relative to the dataset. These differences are visually represented by the color intensity on the heatmap.

This clustering effect suggests that environmental factors such as humidity, temperature, and exposure to UV radiation strongly influence both fungal and bacterial community structures. Additionally, the pigment-producing capabilities of these genera are likely adapted to their respective environments, contributing to biofilm coloration and resilience against environmental stresses.

The green algae *Chlorophyta* include a variety of species capable of synthesizing β-carotene pigment [50]. This is a carotenoid with antioxidant properties and a precursor of vitamin A, and it is widely used in the food, pharmaceutical and cosmetic fields.

These algae are known for their ability to accumulate large amounts of β-carotene under solar irradiation [51]. Their production is a topic of great interest for both scientific research and the biotechnology industry.

The observed differences in microbial profiles across samples are likely influenced by a combination of substrate composition, environmental exposure, and microclimatic

conditions. For instance, samples collected from lime-based substrates, such as L1 and L4, tend to harbor genera like *Rubellimicrobium* and *Truepera*, which are known for their adaptation to calcareous environments. In contrast, synthetic varnish substrates, as in L2 and L3, may select for genera better suited to lower porosity and the potential presence of antimicrobial compounds. Furthermore, the higher moisture levels and prevailing winds in NNW-exposed surfaces could explain the dominance of specific taxa adapted to such conditions. However, the interplay of these factors remains complex, and additional studies are needed to isolate their specific contributions.

Contrary to common belief, microbiological data have revealed that the patina under study is not composed solely of *Trentepohlia*, but rather contains a diverse range of microorganisms, with chlorophyte algae making up only a small fraction. Understanding what kind of biological patina afflicts a building is crucial for several reasons. Each type of biofilm can affect the material in different ways. Some microorganisms can cause direct damage, such as surface decomposition or chemical alteration of the substrate. Knowing the composition of the patina helps to choose the most suitable cleaning treatment to preserve the integrity of the monument without further damaging it. In this case, the concept of prevention, i.e., correctly identifying the type of biological growth, allows more targeted preventive measures to be implemented. Localized biological patinas on external surfaces, as in our case, allow for the monitoring of the building by highlighting pathologies such as rising damp or accidental water leaks that may compromise its conservation.

4. Conclusions

This study provides a comprehensive characterization of red biofilms found on ancient and contemporary buildings in southern Portugal, primarily on carbonate substrates coated with synthetic white varnishes.

The first pink signs of the biofilm are visible in just 2–3 years after the last painting. In 8–10 years, the patina, if not treated, could cover the entire affected wall. Over time, its color increases in intensity based on the thickness of the colonization, reaching burgundy and thicknesses greater than 2 mm. The findings reveal a diverse microbial community structure, with significant variability in composition across samples. The red biofilm coloration is attributed to carotenoid pigments produced by specific microbial taxa such as *Rubellimicrobium* (sample L1) and *Truepera* (samples L2 and L4). However, their presence in specific samples suggests that the overall pigmentation may result from cumulative or synergistic contributions of other taxa or environmental factors. Additionally, the observed differences in microbial community profiles—shaped by substrate properties and environmental exposure (e.g., wall orientation and moisture levels)—highlight the complexity of biofilm formation processes.

The distinct microbial profiles across samples emphasize the influence of local environmental and material conditions on biofilm development. For example, samples with synthetic varnishes (e.g., L2) exhibited different dominant microbial taxa compared to those with lime-based substrates (e.g., L4). These findings suggest that targeted strategies to mitigate biofilm formation should consider both microbial composition and the environmental context. From a practical standpoint, this study underscores the need for tailored biofilm management strategies. Mechanical removal using dry methods (e.g., spatulas) remains an effective approach, especially given the weak adherence of the biofilm. Softwashing techniques with cleaning solutions formulated for microbial removal also show potential, particularly for large-scale applications. For long-term prevention, regular maintenance with biocidal treatments or the use of biocidal paints is recommended, though the latter may pose environmental and cost challenges. Alternatively, the reintroduction of traditional lime-based whitewashing offers a sustainable option for historic buildings, providing both breathability and some degree of biocidal activity. The variability in microbial composition and pigmentation mechanisms across samples highlights the need for further metagenomic analysis to fully understand the interactions between microbial communities, environmental conditions, and substrate characteristics. This understanding will support

the development of more effective and sustainable approaches to managing red biofilms on architectural heritage.

Author Contributions: F.S.: conceptualization, data curation, formal analysis, investigation, project administration, resources, software, supervision, methodology, validation, visualization, writing—original draft, writing—review and editing, C.L.: formal analysis, methodology, validation, visualization, writing—original draft, writing—review and editing L.D.: formal analysis, methodology, validation, writing—review and editing. S.M.A.: formal analysis, methodology, validation, writing—review and editing. A.T.C.: formal analysis, methodology, validation, writing—review and editing. All authors have read and agreed to the published version of the manuscript.

Funding: The authors gratefully acknowledge the European Communion—Portugal, Grant Contract number: Sustainable Stone by Portugal, Call: 2021-C05i0101-02—mobilizing agendas/alliances for reindustrialization—PRR, Proposal: C644943391-00000051.

Data Availability Statement: Data are contained within the article.

Conflicts of Interest: The authors declare no conflicts of interest.

References

1. Caneva, G.; Di Stefano, D.; Giampaolo, C.; Ricci, S.; Kwiatkowski, D.; Löfvendahl, R. Stone Cavity and Porosity as a Limiting Factor for Biological Colonisation: The Travertine of Lungotevere (Rome). In Proceedings of the 10th International Congress on Deterioration and Conservation of Stone, Stockholm, Sweden, 27 June—2 July 2004.
2. Prieto, B.; Young, M.E.; Turmel, A.; Fuentes, E. Role of Masonry Fabric Subsurface Moisture on Biocolonisation. A Case Study. *Build. Environ.* **2022**, *210*, 108690. [CrossRef]
3. Hosseini, Z.; Zangari, G.; Carboni, M.; Caneva, G. Substrate Preferences of Ruderal Plants in Colonizing Stone Monuments of the Pasargadae World Heritage Site, Iran. *Sustainability* **2021**, *13*, 9381. [CrossRef]
4. Elgohary, Y.M.; Mansour, M.M.A.; Salem, M.Z.M. Assessment of the Potential Effects of Plants with Their Secreted Biochemicals on the Biodeterioration of Archaeological Stones. *Biomass Convers. Biorefinery* **2024**, *14*, 12069–12083. [CrossRef]
5. Del Monte, M. Ll Biodegrado Dei Monuementi in Pietra: I Licheni e i "Segni El Tempo". *Il Geol. Dell'emilia Romagna* **2007**, *7*, 11–55.
6. Jain, A.; Bhadauria, S.; Kumar, V.; Chauhan, R.S. Biodeterioration of Sandstone under the Influence of Different Humidity Levels in Laboratory Conditions. *Build. Environ.* **2009**, *44*, 1276–1284. [CrossRef]
7. Hauck, M.; Jürgens, S.R. Usnic Acid Controls the Acidity Tolerance of Lichens. *Environ. Pollut.* **2008**, *156*, 115–122. [CrossRef]
8. Song, J.; Ru, J.; Zhang, H.; Cao, K.; Cui, X. Research Progress on Lichens, Lichenic Acids, Rock and Mineral Weathering and Its Mechanisms. *J. Nanjing For. Univ. (Nat. Sci. Ed.)* **2019**, *62*, 169. [CrossRef]
9. Rundel, P.W. The Ecological Role of Secondary Lichen Substances. *Biochem. Syst. Ecol.* **1978**, *6*, 157–170. [CrossRef]
10. Haas, J.R.; Purvis, O.W. Lichen Biogeochemistry. In *Fungi in Biogeochemical Cycles*; Cambridge University Press: Cambridge, UK, 2006; ISBN 9780511550522.
11. Schatz, A. Pedogenic (Soil-Forming) Activity of Lichen Acids. *Naturwissenschaften* **1962**, *49*, 518–519. [CrossRef]
12. Gadd, G.M.; Bahri-Esfahani, J.; Li, Q.; Rhee, Y.J.; Wei, Z.; Fomina, M.; Liang, X. Oxalate Production by Fungi: Significance in Geomycology, Biodeterioration and Bioremediation. *Fungal Biol. Rev.* **2014**, *28*, 36–55. [CrossRef]
13. Lisci, C.; Pires, V.; Sitzia, F.; Mirão, J. Limestones Durability Study on Salt Crystallisation: An Integrated Approach. *Case Stud. Constr. Mater.* **2022**, *17*, e01572. [CrossRef]
14. Sitzia, F.; Beltrame, M.; Columbu, S.; Lisci, C.; Miguel, C.; Mirão, J. Ancient Restoration and Production Technologies of Roman Mortars from Monuments Placed in Hydrogeological Risk Areas: A Case Study. *Archaeol. Anthropol. Sci.* **2020**, *12*, 147. [CrossRef]
15. Isola, D.; Bartoli, F.; Meloni, P.; Caneva, G.; Zucconi, L. Black Fungi and Stone Heritage Conservation: Ecological and Metabolic Assays for Evaluating Colonization Potential and Responses to Traditional Biocides. *Appl. Sci.* **2022**, *12*, 2038. [CrossRef]
16. Tyagi, P.; Verma, R.K.; Jain, N. Fungal Degradation of Cultural Heritage Monuments and Management Options. *Curr. Sci.* **2021**, *121*, 1553–1560. [CrossRef]
17. Sitzia, F.; Lisci, C.; Pires, V.; Dias, L.; Mirao, J.; Caldeira, A.T. Predicted Dynamic of Biodeterioration in Cultural Heritage Stones Due to Climate Changes in Humid Tropical Regions—A Case Study on the Rhodotorula Sp. Yeast. *Heritage* **2023**, *6*, 7727–7741. [CrossRef]
18. Gómez-Bolea, A.; Llop, E.; Ariño, X.; Saiz-Jimenez, C.; Bonazza, A.; Messina, P.; Sabbioni, C. Mapping the Impact of Climate Change on Biomass Accumulation on Stone. *J. Cult. Herit.* **2012**, *13*, 254–258. [CrossRef]
19. Cutler, N.A.; Oliver, A.E.; Viles, H.A.; Ahmad, S.; Whiteley, A.S. The Characterisation of Eukaryotic Microbial Communities Onsandstone Buildings in Belfast, UK, Using TRFLP and 454 Pyrosequencing. *Int. Biodeterior. Biodegrad.* **2013**, *82*, 124–133. [CrossRef]
20. Mokrzycki, W.; Tatol, M. Color Difference Delta E—A Survey. *Mach. Graph. Vis.* **2012**, *20*, 383–411.

21. Durgenova, A.; Piksayakina, A.; Bogatov, V.; Salman, A.L.; Erofeev, V. The Economic Damage from Biodeterioration in Building Sector. *IOP Conf. Ser. Mater. Sci. Eng.* **2019**, *698*, 077020. [CrossRef]
22. Martins, J.P.; Madalena, B.; De Souza, M.; Óscar, A.; Levy, M. *O Caminho de Ferro Revisitado: O Caminho de Ferro Em Portugal de 1856 a 1996*; Caminhos de Ferro Portugueses: Lisbon, Portugal, 1996.
23. Miguel, L. *As Ruas Da Vila de Arraiolos*; Câmara de Arraiolos: Arraiolos, Portugal, 2021.
24. Espanca, T. *Inventário Artístico de Portugal: Concelho de Évora*; Academia Nacional de Belas-artes: Lisbon, Portugal, 1966.
25. Rosado, T.; Dias, L.; Lança, M.; Nogueira, C.; Santos, R.; Martins, M.R.; Candeias, A.; Mirão, J.; Caldeira, A.T. Assessment of Microbiota Present on a Portuguese Historical Stone Convent Using High-Throughput Sequencing Approaches. *Microbiologyopen* **2020**, *9*, 1067–1084. [CrossRef] [PubMed]
26. Dias, L.; Rosado, T.; Candeias, A.; Mirão, J.; Caldeira, A.T. A Change in Composition, a Change in Colour: The Case of Limestone Sculptures from the Portuguese National Museum of Ancient Art. *J. Cult. Herit.* **2020**, *42*, 255–262. [CrossRef]
27. Dhariwal, A.; Chong, J.; Habib, S.; King, I.L.; Agellon, L.B.; Xia, J. MicrobiomeAnalyst: A Web-Based Tool for Comprehensive Statistical, Visual and Meta-Analysis of Microbiome Data. *Nucleic Acids Res.* **2017**, *45*, W180–W188. [CrossRef] [PubMed]
28. Henriques, F.; Charola, A.E.; Moreira Rato, V.; Faria Rodrigues, P. Development of Biocolonization Resistant Mortars: Preliminary Results. *Restor. Build. Monum. Int. J. Bauinstandsetz. Baudenkmalpfl. Int. Zeitschrift* **2007**, *13*, 389–400.
29. Columbu, S.; Palomba, M.; Sitzia, F.; Carcangiu, G.; Meloni, P. Pyroclastic Stones as Building Materials in Medieval Romanesque Architecture of Sardinia (Italy): Chemical-Physical Features of Rocks and Associated Alterations. *Int. J. Archit. Herit.* **2020**, *16*, 49–66. [CrossRef]
30. Alhawari, A.; Mukhopadhyaya, P. Thermal Bridges in Building Envelopes—An Overview of Impacts and Solutions. *Int. Rev. Appl. Sci. Eng.* **2018**, *9*, 31–40. [CrossRef]
31. Argiolas, M. *L'umidità Da Risalita Muraria. Diagnosi e Sistemi Correttivi. Edizione Ampliata*; Maggioli Editore, Ed.; Maggioli Editore: Santarcangelo di Romagna, Italy, 2020; ISBN 978-8891640031.
32. Argiolas, M. *Muffe e Condense Negli Edifici: Diagnosi e Sistemi Correttivi*; I.; Maggioli: Santarcangelo di Romagna, Italy, 2020; ISBN 8891641335.
33. Smith, B. *Infrared Spectral Interpretation: A Systematic Approach*; CRC Press: Boca Raton, FL, USA, 2018; ISBN 9781351438384.
34. Wiley, S. Spectrabase ®. Available online: https://spectrabase.com (accessed on 1 December 2024).
35. Lóránd, T.; Deli, J.; Molnár, P.; Tóth, G. FT-IR Study of Some Carotenoids. *Helv. Chim. Acta* **2002**, *85*, 1691–1697. Available online: https://onlinelibrary.wiley.com/doi/10.1002/1522-2675(200206)85:6%3C1691::AID-HLCA1691%3E3.0.CO;2-G (accessed on 1 October 2024).
36. Saito, T.; Terato, H.; Yamamoto, O. Pigments of Rubrobacter Radiotolerans. *Arch. Microbiol.* **1994**, *162*, 414–421. [CrossRef]
37. Jurado, V.; Miller, A.Z.; Alias-Villegas, C.; Laiz, L.; Saiz-Jimenez, C. Rubrobacter Bracarensis Sp. Nov., a Novel Member of the Genus Rubrobacter Isolated from a Biodeteriorated Monument. *Syst. Appl. Microbiol.* **2012**, *35*, 306–309. [CrossRef] [PubMed]
38. Gorbushina, A.A. Life on the Rocks. *Environ. Microbiol.* **2007**, *9*, 1613–1631. [CrossRef] [PubMed]
39. Jebbar, M.; Hickman-Lewis, K.; Cavalazzi, B.; Taubner, R.S.; Rittmann, S.K.M.R.; Antunes, A. Microbial Diversity and Biosignatures: An Icy Moons Perspective. *Space Sci. Rev.* **2020**, *216*, 10. [CrossRef]
40. Dyda, M.; Laudy, A.; Decewicz, P.; Romaniuk, K.; Ciezkowska, M.; Szajewska, A.; Solecka, D.; Dziewit, L.; Drewniak, L.; Skłodowska, A. Diversity of Biodeteriorative Bacterial and Fungal Consortia in Winter and Summer on Historical Sandstone of the Northern Pergola, Museum of King John III's Palace at Wilanow, Poland. *Appl. Sci.* **2021**, *11*, 620. [CrossRef]
41. Romano-Bertrand, S.; Bourdier, A.; Aujoulat, F.; Michon, A.L.; Masnou, A.; Parer, S.; Marchandin, H.; Jumas-Bilak, E. Skin Microbiota Is the Main Reservoir of Roseomonas Mucosa, an Emerging Opportunistic Pathogen so Far Assumed to Be Environmental. *Clin. Microbiol. Infect.* **2016**, *22*, 737.e1–737.e7. [CrossRef] [PubMed]
42. Wu, F.; Zhang, Y.; He, D.; Gu, J.D.; Guo, Q.; Liu, X.; Duan, Y.; Zhao, J.; Wang, W.; Feng, H. Community Structures of Bacteria and Archaea Associated with the Biodeterioration of Sandstone Sculptures at the Beishiku Temple. *Int. Biodeterior. Biodegrad.* **2021**, *164*, 105290. [CrossRef]
43. Busse, H.J. Review of the Taxonomy of the Genus Arthrobacter, Emendation of the Genus Arthrobacter Sensu Lato, Proposal to Reclassify Selected Species of the Genus Arthrobacter in the Novel Genera Glutamicibacter Gen. Nov., Paeniglutamicibacter Gen. Nov., Pseudogluta. *Int. J. Syst. Evol. Microbiol.* **2016**, *66*, 9–37. [CrossRef] [PubMed]
44. Chauhan, A.; Pathak, A.; Jaswal, R.; Edwards, B.; Chappell, D.; Ball, C.; Garcia-Sillas, R.; Stothard, P.; Seaman, J. Physiological and Comparative Genomic Analysis of Arthrobacter Sp. SRS-W-1-2016 Provides Insights on Niche Adaptation for Survival in Uraniferous Soils. *Genes* **2018**, *9*, 31. [CrossRef] [PubMed]
45. Li, Q.; Zhang, B.; Yang, X.; Ge, Q. Deterioration-Associated Microbiome of Stone Monuments: Structure, Variation, and Assembly. *Appl. Environ. Microbiol.* **2018**, *84*, 2680–2687. [CrossRef]
46. Avalos, J.; Carmen Limón, M. Biological Roles of Fungal Carotenoids. *Curr. Genet.* **2015**, *61*, 309–324. [CrossRef] [PubMed]
47. Grube, M.; Wedin, M. Lichenized Fungi and the Evolution of Symbiotic Organization. *Microbiol. Spectr.* **2016**, *4*, 749–765. [CrossRef]
48. Crous, P.W.; Wingfield, M.J.; Guarro, J.; Sutton, D.A.; Acharya, K.; Barber, P.A.; Boekhout, T.; Dimitrov, R.A.; Dueñas, M.; Dutta, A.K.; et al. Fungal Planet Description Sheets. *Persoonia* **2015**, *34*, 167–266. [CrossRef] [PubMed]
49. Sterflinger, K. Fungi: Their Role in Deterioration of Cultural Heritage. *Fungal Biol. Rev.* **2010**, *24*, 47–55. [CrossRef]

50. Saad Al-Khafaji, A.; Al-Tae, I.A. Effect of Environmental Factors on β-Carotene Production in Green Algae—A Review. *Chem. Environ. Sci. Arch.* **2023**, *3*, 48–54. [CrossRef]
51. Gómez, P.I.; González, M.A. The Effect of Temparature and Irradiance on the Growth and Carotenogenic Capacity of Seven Strains of *Dunaliella salina* (Chlorophyta) Cultivated under Laboratory Conditions. *Biol. Res.* **2005**, *38*, 151–162. [CrossRef]